Available online at www.sciencedirect.com

SCIENCE DIRECT®

Journal of Electrocardiology 38 (2005) 87–94

JOURNAL OF Electrocardiology

www.elsevier.com/locate/jelectrocard

The effect of intrathoracic heart position on electrocardiogram autocorrelation maps

Alexandru D. Corlan, MD, PhD[a], Robert S. Macleod, PhD[b], Luigi De Ambroggi, MD, FESC[c,*]

[a]*Academy of Medical Sciences, University Hospital of Bucharest, 050098 Bucharest, Romania*
[b]*Cardiovascular Research and Training Institute (CVRTI), University of Utah, Salt Lake City, UT 84112, USA*
[c]*Department of Cardiology, Istituto Policlinico San Donato, University of Milan, 20097 San Donato Milanese, Italy*

Received 16 June 2004; revised 1 October 2004; accepted 1 October 2004

Abstract We studied the influence of the heart position in the thorax on the autocorrelation (AC) maps consisting of correlation coefficients between each pair of instantaneous electrocardiogram potential distributions over a time interval. We used a thorax-shaped electrolytic-filled tank with an isolated and perfused dog heart placed at positions spanning 5 cm on each space direction.The correlation coefficient between QRST AC maps was in the range of 0.92 to 0.99, whereas the correlation coefficient between the corresponding QRST integral maps was in the range of 0.55 to 0.87, proving that AC maps are less influenced by the heart position than integral maps.Thus, diagnostic indexes computed from the AC maps can be expected to be more specific to phenomena taking place in the myocardium than to criteria based directly on electrocardiogram amplitudes in various leads.

Keywords: Body surface ECG maps; Autocorrelation maps; Langendorf preparation; Dog heart; Forward problem of the ECG

1. Introduction

Body surface potential patterns are influenced by the properties of the volume conductor, in particular, the geometry of the thorax and the position of the heart in the thorax [1-4]. A recent study by MacLeod et al [5] demonstrated that variability of the geometric position of the heart in the thorax may cause changes in body surface potentials that exceed diagnostic thresholds for pathological conditions.

We previously proposed indexes of repolarization heterogeneity that were based on correlations between instantaneous potentials during the cardiac cycle [6-9]. These indexes detect subtle features of the spatiotemporal distribution of body surface potentials that may be associated with a substrate favorable to ventricular arrhythmias. Theoretically, these indexes should be independent of the amplitude of the potentials and of the characteristic of the volume conductor (chest geometry, heart position), as illustrated in Fig. 1 and explained in the Appendix.

However, assumptions under which the theory holds are only approximately met in an experimental setting because the potential on surfaces around the heart are only sampled at a finite number of points (where the electrocardiogram [ECG] electrodes are placed) and the heart moves during the cardiac cycle.

The purpose of this study was to assess the accuracy of the theoretical expectation that correlation coefficients between instantaneous potentials are invariant to the geometry of the volume conductor between the heart and the lead system. Preliminary results have been recently reported in abstract form [10].

2. Methods

2.1. Experimental preparation

We used data obtained in a previous experiment, performed at the Cardiovascular Research and Training Institute, University of Utah, and previously reported [5]. In short, isolated dog hearts, perfused by blood from another (support) dog, were immersed in a human torso–shaped tank and were filled with electrolyte. Electrograms were obtained

* Corresponding author. Tel.: +39 2 527 74 520; fax: +39 2 527 74 520.
E-mail address: luigi.deambroggi@unimi.it (L. De Ambroggi).

0022-0736/$ – see front matter © 2005 Elsevier Inc. All rights reserved.
doi:10.1016/j.jelectrocard.2004.10.006

from 370 electrodes on the interior surface of the tank and 128 electrodes sewn in a stocking over the ventricles.

The heart was moved in 1-cm steps on the horizontal axis (x-axis) over a range of 6 cm, on the anteroposterior axis (y-axis) over a range of 5 cm, and on the vertical axis (z-axis) over a range of 5 cm.

For each position, the heart preparation was paced in the right atrium and at least 1 cardiac cycle was recorded. The spatial positions of the electrodes on both the epicardial sock and the tank were digitized at the end of the experiment. The detailed procedure has been described [5].

2.2. Beat selection and processing

From each recording, we manually selected 1 beat and split the leads into 2 simultaneous sets (tank leads and epicardial leads) and performed baseline correction. One lead from the epicardial stocking that was noisy in some of the recordings was eliminated (ie, not replaced) in all of them.

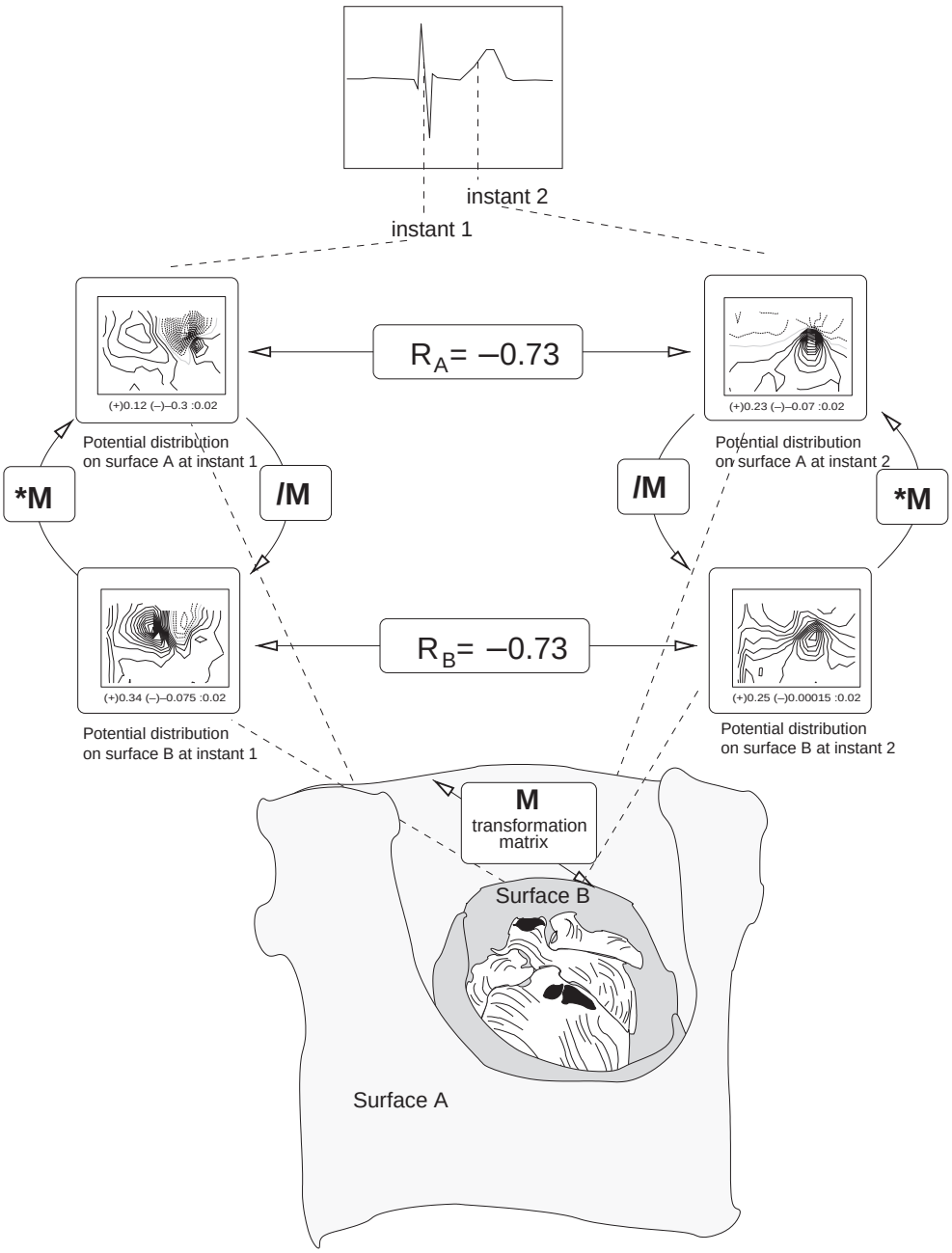

Fig. 1. The principle of the invariance of the AC map with the volume conductor. Given 2 closed surfaces, A and B, each of them completely surrounding the myocardium and at some distance from it, there is a unique invertible matrix **M**, such that at a given instant, the potentials on surface A can be obtained by matrix multiplication between those at the same instance on surfaces B and M. This linear transform preserves the correlation coefficient unchanged between instantaneous potential distributions at the same instants before and after transformation. R_A and R_B indicate correlation coefficients between instantaneous potential distributions at the same 2 time instants on surfaces A and B, respectively.

To align beats across different recordings, we selected, as a reference, the peak of the root-mean-square computed from all the epicardial leads and then selected a QRS window extending from 29 milliseconds before to 30 milliseconds after the reference. The ST-T interval similarly extended from the end of the QRS window to 172 milliseconds after the reference, and we assumed that these temporal fiducials applied globally to all epicardial and torso tank leads. The fiducials determined the time windows for the integral maps described in the next section.

2.3. Instantaneous and integral maps

Visualization of the recorded data consisted of both series of instantaneous potential distributions over the heart and torso tank surfaces as well as a set of integral maps typically used in this field computed using the fiducial markers. The QRS, QRST, and ST-T integral maps were obtained by calculating for each lead the sum of all instantaneous potentials on the lead in the respective interval multiplied by the sampling interval. To display these maps, we projected the 3-dimensional measurement lead locations of the torso tank to a rectangle in a 2-step process. First, we determined the direction from the centroid of the tank to each point on the surface and then mapped each to a rectangle in which the horizontal angle appeared on the x-axis and the vertical angle on the y-axis. Then, to create a regular grid of data points in the rectangle, we carried out bilinear interpolation using the immediately neighboring measured values.

2.4. Autocorrelation maps

According to Abildskov et al [11], to obtain autocorrelation (AC) maps, the cross-correlation between each instantaneous surface map in the original data and each of the other instantaneous map in the same leads is computed. We naturally separated epicardial maps from tank surface maps and thus ended up with 2 sets of correlation values for each beat.

The result for each beat was a matrix with 201 rows and 201 columns (the number of samples during the QT interval), 1 row and 1 column for each instant in the QT interval. The elements of the matrix are numbers between −1.0 and 1.0—the correlation coefficients between potential distribution at the instants represented by the column and the row of the element. The values on the main diagonal (where row number equals column number) are always 1.0 because they represent the correlation of a potential distribution with itself. The matrix is symmetric with respect to the main diagonal because the correlation between potential distributions at moments, say, t_0 and t_1, equal that between t_1 and t_0. This matrix is called the AC map of the QT interval, and in all, we obtained 36 maps (18 for the tank surface recordings and 18 for the corresponding epicardial recordings), each pair corresponding to a different heart location.

We displayed AC maps, as in Fig. 2, in which each point represents the correlation coefficient between the potential distribution at the instants at its x and y coordinates (column and row indexes). The value of the correlation coefficient is

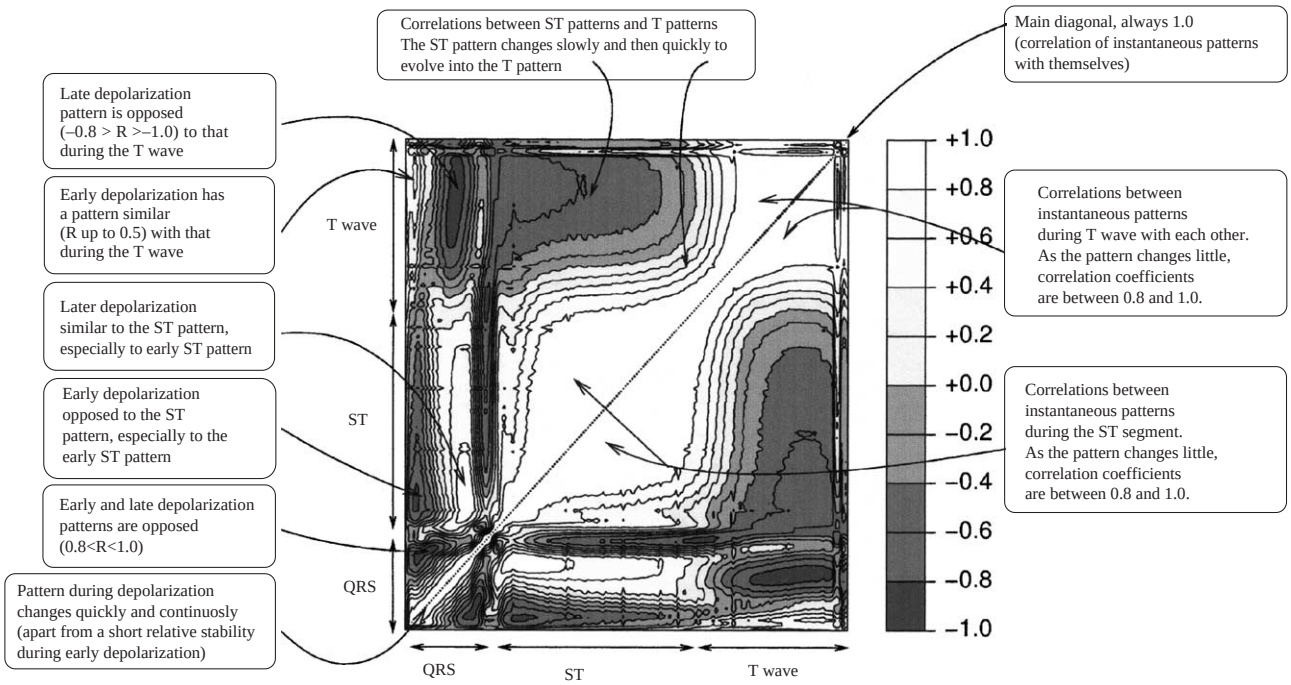

Fig. 2. AC map of 1 cardiac beat. Successive instants during the QT interval of the same cardiac cycle are on both x and y. Each point on the map represents the correlation coefficient between instantaneous potential distributions at the instants corresponding to the points' x and y coordinates (the column and row of the autocorrelation matrix). The scale at the right of the figure shows how correlation coefficients are represented as shades of gray.

represented by the shade of gray of the point, from black (for −1.0) to white (for 1.0), as shown in the scale at the right of the map. The main diagonal (which represents correlation coefficients between 0.8 and 1.0) appears in white. To the left and right of the main diagonal, the correlation coefficients generally lay between 1.0 and 0.8, indicating relatively little change in neighboring time instants, as one would expect. The width of the white

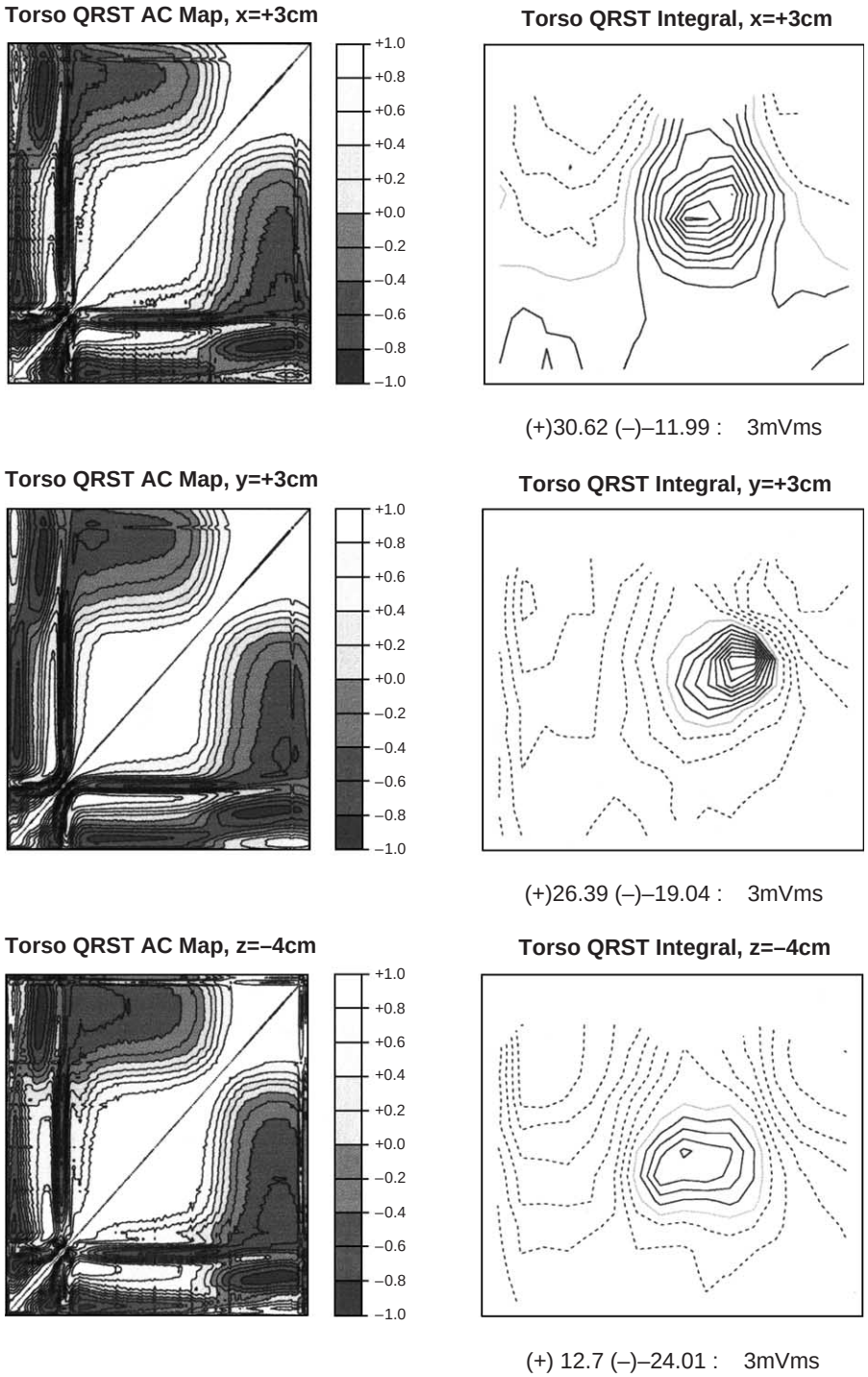

Fig. 3. AC maps (left column) vs QRST integrals (right column) derived from the measurements of potential from the surface of the torso tank of the same cardiac cycles. Potentials were recorded with the heart at the most distant positions from the control point (3 cm on x, 3 cm on y, and −4 cm on z). The higher variability of the integral maps is evident. AC maps are described in Fig. 2. For the integral maps, the left half represents the anterior face of the thorax-shaped tank while the right half represents the posterior face. Lines are isointegrals with 3 mV · milliseconds between lines. Continuous lines are for positive integral values; dashed lines are for negative integral values; the gray line represents the 0 isointegral line. The legend marked (+) represents the maximum value on the tank; (−), the minimum value (with all values in mV · milliseconds).

region around the main diagonal at a given instant is then inversely proportional to the rate of the pattern change at that instant. During depolarization, the white area is markedly thinner (because the rate of change was high); a second, less extensive narrowing was visible in the region corresponding to the J point, where the S wave transitions to ST segment. Large white regions represent the correlation between slowly changing instantaneous patterns during the ST segment and the T wave, respectively.

More generally, each point in the map describes the correlational relationship between the signals measured at 2 different instants during the heart beat.

2.5. Distance between 2 maps

We have used 2 different metrics for the extent of the difference between maps recorded from different heart positions in the torso tank. For integral maps (sums of the potentials over an interval such as the QRS), we used pairwise correlation between the measured maps for each of different intervals. For AC maps, the correlation between corresponding points on pairs of maps provided an analogous metric for similarity between AC values at different heart locations.

3. Results

As expected and previously reported [5], there was little variation in the epicardial potentials for any changes in the heart location in the tank. This suggests a very stable preparation and supports the assumption that all changes in torso tank potentials originate from variations in heart/torso geometry.

Fig. 3 contains AC (left column) and QRST (right column) integral maps measured from the torso tank for the most distant (relative to the reference location) positions of the heart. Immediately evident from viewing the maps is the fact that AC maps did not vary across heart positions nearly to the extent of the integral maps.

To quantify the location-induced differences that arose among AC maps and those between the integral maps, we considered the series of displacements along the 3 directions. The recording at x = 3 cm was taken as the baseline for movements in x (in 1-cm steps to −2 cm), with y = 4 cm as the baseline for movements in y and z = 0 cm as the baseline for movements in z. For each displacement step on the 3 directions, the distance of the AC map at that position from the AC map of the baseline was measured using the correlation coefficient between them; the same was applied to the corresponding integral maps of the 2 recordings.

Fig. 4 shows the results of performing this procedure for QRS integral maps and AC maps of the QRS (top panel), for ST-T integral maps and AC maps of the ST-T interval (middle panel), and for QRST integral maps and the whole QRST AC maps (lower panel).

The deviation from the baseline recording was much higher in integral maps than in AC maps.

Although the correlation between AC maps was high (above 0.95 in most cases), there was a slight deviation from the baseline aspect that was, to some extent, proportional to the geometrical displacement. This relationship appeared more pronounced in the ST-T AC maps and the QRST AC maps (which include both the QRS and the ST-T) than in the QRS AC maps.

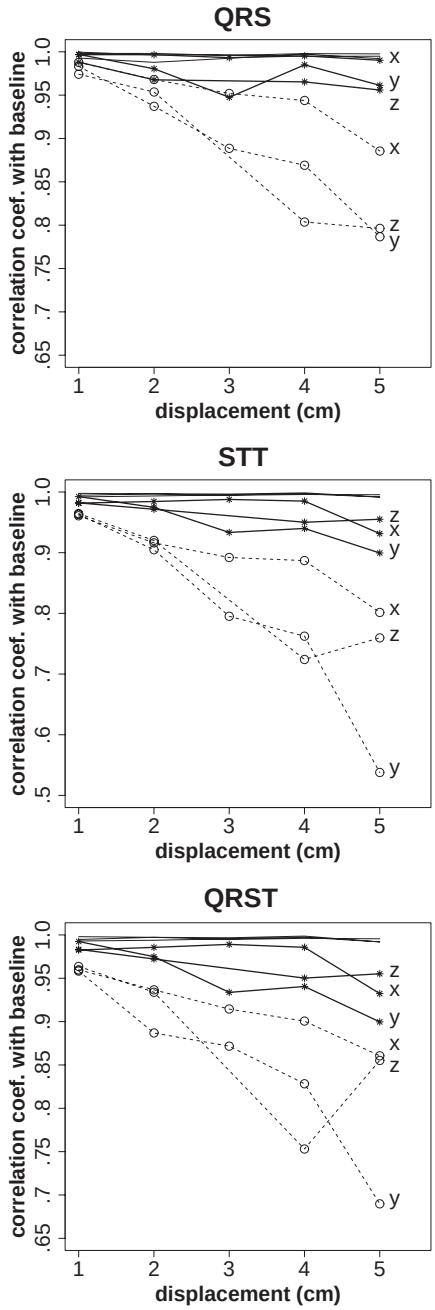

Fig. 4. Correlation coefficients between the baseline map and successive maps in the x, y, and z displacement series. The thin continuous lines, which appear at the top of each panel, are for AC maps on the epicardial sock, thick continuous lines for AC maps on the tank, and dashed lines for integral maps of the same recordings. The QRS AC maps and integral maps are considered in the upper panel, the STT in the middle panel, and the QRST in the lower panel.

To quantify the variability in various regions of the AC map as a function of the position of the heart in the tank, we considered the AC maps of all tank recordings produced during the experiment and synchronized by the instant of the maximum value of the root-mean-square on the epicardial leads. For each point (pair of intervals relative to the synchronization instant) in all maps, we computed the SD of the values found in all maps, obtaining a dispersion map of the AC maps. This procedure was performed separately for the tank leads (Fig. 5, top) and for the epicardial leads (Fig. 5, bottom).

For the tank AC maps, the average of the whole deviation map was 0.105; for the QRS region, 0.095; for the ST-T region, 0.091; for the early repolarization vs late repolarization, 0.133; whereas for the depolarization vs repolarization, 0.122. For the epicardial maps, the average of the deviation map was 0.032 for the whole map, 0.039 for the QRS region, 0.020 for the ST-T region, 0.029 for the early repolarization vs late repolarization, and 0.046 for the depolarization region vs repolarization region. The correlation between epicardial and the corresponding tank surface AC maps was relatively low: 0.72 ± 0.045 for the whole map, 0.86 ± 0.017 for the QRS region, and 0.87 ± 0.024 for the ST-T region.

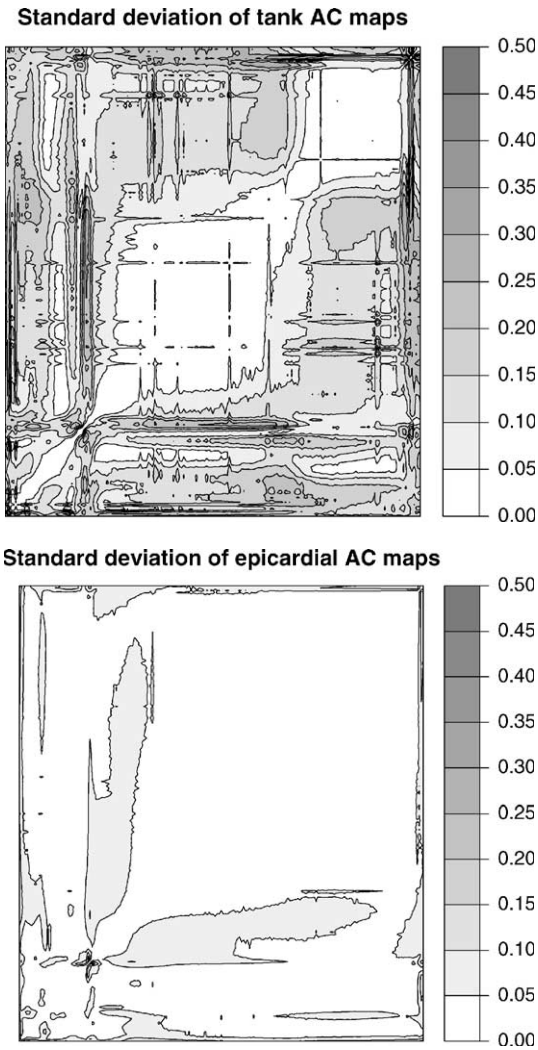

Fig. 5. Dispersion of the correlation coefficients at the same pairs of instants across all atrial-paced cardiac cycles recorded in the experiment for the recordings on the torso tank (top panel) and the epicardial sock (bottom panel).

4. Discussion

A factor contributing to the lack of diagnostic accuracy of body surface ECG measurements is the influence of the interindividual and intraindividual variability of the thorax conductor through which the myocardial electrical activity is measured. It can be expected that by extracting from the ECG potentials only the information reflecting phenomena in the ECG source (myocardium), more specific diagnostic indexes could be developed. Such indexes are particularly needed for the identification of electrical disturbances associated with the risk of malignant ventricular arrhythmias.

Because the thorax is a purely resistive conductor [12,13], potentials at the body surface can be obtained from those on the epicardium by a linear transformation. The correlation coefficient between potential distributions at any 2 instants should not depend on the transformation matrix (properties of the thorax conductor) but only on the ECG source.

For example, if the same distribution of current dipoles is present in the myocardium at 2 instants in time, the potential distributions on the body surface will depend on the thorax geometry but will be identical at the 2 instants, and the correlation coefficient between potentials at the 2 instants will be 1, irrespective of the thorax geometry. The assumptions under which the same is true for any pair of current dipole distributions are presented in the Appendix.

In this study we tried to verify the accuracy of the independence of the matrix of correlation coefficients between every 2 instantaneous distributions in an ECG interval (AC maps), which may be limited by the heart contraction and rotation during the ST-T interval and by the fact that the ECG is measured with a finite number of electrodes.

We used a set of single-beat recordings obtained on a 370-lead system on a human torso–shaped tank in which the same dog heart was placed at various geometrical displacements.

The AC maps showed substantially less variability than the integral maps (QRS, ST-T, or QRST) calculated from the same recordings.

However, AC maps on the tank showed more variability than those on the epicardium, especially in the regions constructed from the correlation of early repolarization vs late repolarization and of QRS vs ST-T.

Variation of the AC map when the heart is moved inside the tank, although limited, reflects a degree of dependence of the AC map on the volume conductor between myocardium and tank. Two phenomena could explain this: (1) the heart moves during the recording and (2) the instantaneous potential distributions, as recorded, are only

approximations of potential distributions on continuous closed surfaces around the heart.

Heart movements related to ventricular contraction are usually ignored in electrocardiography because their effect is supposed to contribute little to the general variability of the ECG signals. However, recent studies evaluating the contribution of thoracic variability to the variability of the body surface ECG 2 to 5 only concentrate on the depolarization, possibly to avoid the influence of heart contraction on the results. Contraction and rotation are most important during early repolarization and diminish in amplitude over the T wave. Thus, the position of the heart can be considered to be essentially unchanged over the QRS and to change gradually over the ST. This is consistent with our finding of higher variability of the AC map in the regions opposing early to late repolarization and repolarization to depolarization, respectively. In these regions, the deviation map is about 0.125, whereas over the QRS, for example, it is about 0.095. This suggests that movements of the heart could account for about 30% of the variation of the AC map in the regions corresponding to the ST-T interval. The presence of increased variability in the same interval in epicardial maps further supports the hypothesis that it is caused by heart movements.

Another 20% to 30% of the difference in AC maps must be attributed to actual variability of the ECG source itself, as illustrated by the variability of the AC maps on the epicardial recordings.

The rest of the AC map variability on the body surface could be attributed to the imprecision with which the lead system used approximates the potential distributed continuously on a closed surface around the heart. This explanation is also consistent with the results of Hoekema et al [1,14], who found that transforming potentials between 2 lead systems can incur a relative difference of up to 10% to 20% (measured with the relative difference metric, corresponding to $r = 0.99$-0.98).

The minimum number of electrodes that can provide a reasonable approximation of the AC map is likely related to the complexity of the instantaneous potential distribution patterns. In a previous investigation [15], the AC map reconstructed from 3 pairs of electrodes in orthogonal directions reproduced the main features of the AC map constructed from 62 body surface electrodes when potential distributions were dipolar but were substantially different when the distribution was multipolar, as during the breakthrough of depolarization through the ventricular wall and around the J point.

Consistent with the above observations, Fig. 5 shows that around the J point, the dispersion of the AC map in this experiment was also slightly higher, both on the epicardial and tank recordings.

The results in this study have essentially reproduced, in an experimental setting, the results of a previous simulation study [16] that found correlations between AC maps of 0.95 to 1.0 for lead systems that were displaced or rotated with respect to the simulated myocardium.

We see 2 practical implications of our observations: (1) diagnostic indexes and criteria that are derived from the AC maps [6-9] can be expected to be less influenced by interindividual variations in thorax geometry than indexes and criteria that are based on wave amplitudes and derivatives; (2) computer models of the myocardial activation and repolarization may be compared with real recordings in terms of AC maps without the need to include the features of the thorax.

4.1. Conclusion

ECG AC maps show much lower variation with the geometry of the volume conductor between the myocardium and the lead system than other representations of the ECG such as integral maps. Thus, diagnostic indexes computed from the ECG AC maps can be expected to be more specific to phenomena taking place in the myocardium than criteria based directly on ECG amplitudes in various leads.

Acknowledgments

The authors thank Ileana Corlan, MD, for comments on the manuscript and Radu Corlan, BSEE, for helpful discussions regarding the mathematical implications of the electrical properties of volume conductors.

Appendix

Given 2 sets of points in a purely resistive conductor medium, the potentials on 1 set can be computed from those on the other set by a linear transform (multiplying the first set with a matrix). The transformation matrix is specific to the conductor between the electrode sets.

In other terms, let A and B be 2 sets of N electrodes, each in a volume conductor. There is a unique matrix, $\mathbf{M}$, such that given potentials A_0 at instant t_0 on lead set A, potentials on lead set B at the same instant are given by

$$B_0 = A_0\mathbf{M}.$$

Provided that $\mathbf{M}$ admits an inverse and considering 2 instants (t_1, t_2) in time, the correlation coefficient between the potentials on 1 set of electrodes at the 2 instants equals the correlation between potentials on the other set at the same instants:

$$cor(A_1,A_2) = cor(A_1\mathbf{M},A_2\mathbf{M}) = cor(B_1,B_2).$$

The need for matrix $\mathbf{M}$ to be invertible is illustrated by the fact that the reverse form of the above equation,

$$cor(B_1,B_2) = cor\left(B_1\mathbf{M}^{-1},B_1\mathbf{M}^{-1}\right) = cor(A_1,A_2),$$

must also hold; thus both $\mathbf{M}$ and $\mathbf{M}^{-1}$ must exist. In electrocardiography, the above statement is valid if A and B are potential distributions on completely closed, nonintersecting surfaces around the heart.

The immediate implication of the above is that even if we do not know the matrix **M** but we know it is invertible, by determining the correlation coefficient between instantaneous potentials on a surface around the heart (eg, on the thorax) at 2 instants in time, we also know its value on any other surface; or, in other terms, that the correlation coefficient between instantaneous potentials does not depend on the surface chosen for the measurement of the potentials but only on the features of the ECG source.

This method is fully exploited by recording a complete cardiac cycle, computing the correlation between potentials at every pair of samples, and displaying the square matrix of the results as a map (with the same time interval on both x and y and correlations between every 2 instants as points on the map of corresponding gray intensity), called an "autocorrelation map." In other terms, if a cardiac cycle occurs between instants t_{start} and t_{end} and A is the lead system on which potentials are measured, A_x being the potentials obtained at moment x, the AC map is the function ρ defined as

$$\rho(\mathrm{x,y}):[t_{\mathrm{start}},t_{\mathrm{end}}]\times[t_{\mathrm{start}},t_{\mathrm{end}}]\rightarrow[-1,1],\ \rho(\mathrm{x,y})=\mathrm{cor}\left(A_{\mathrm{x}},A_{\mathrm{y}}\right).$$

This application relies on 2 assumptions: (1) matrix **M** is the same at the 2 instants; in other words, the heart does not move with respect to either of the lead systems A and B and (2) it is invertible. The first assumption is only approximately true because the heart contracts, pendulates, and rotates to some extent during the ST-T interval. However, at least in the tank experiment, this only had a limited contribution to the variability of the AC maps determined on the tank, as discussed in the main article.

According to the bidomain model [17], an exact description of the ECG source would be provided by the potential distribution on a closed surface around the myocardium covering the epicardium, the mitral and tricuspid rings, and the endocardium. An infinity of potentials, 1 for every point on the surface, would be needed to fully describe the source. However, any lead system used in practice will only have a finite number of electrodes. The instantaneous potential distribution effectively collected will only provide an approximation of the potential distribution on the respective surface, and thus the correlation coefficients between pairs of potential distributions will also represent approximations.

These approximations will be influenced by the number of electrodes, by their placement, and by the properties of the instantaneous potential distributions. A simpler potential distribution, such as a dipolar one, will be adequately approximated by even a small number of electrodes, as illustrated in [15]. A special case is represented by the epicardial lead system, especially as it does not cover the endocardium or the complete heart. Leads very close to the epicardium, much closer than the thickness of the ventricular wall, or the interelectrode distance, will reflect primarily the potential right under the electrode, whereas potentials on the source, surface further from the electrode, will provide a very small contribution. Thus, electrode systems that are very close to the myocardium, especially if not covering it completely, will lead to AC maps that are substantially different from AC maps obtained at some distance from the heart, as shown in this study and in the study of Corlan et al [16].

References

[1] Hoekema R, Huiskamp G, Oostendorp T, Uijen GJH, van Oosterom A. Lead system transformation for pooling of body surface map data: a surface Laplacian approach. J Electrocardiol 1995;28:344.

[2] Hoekema R, Uijen GJH, van Erning L, van Oosterom A. Interindividual variability of multilead electrocardiographic recordings: influence of heart position. J Electrocardiol 1999;32:137.

[3] van Oosterom A, Hoekema R, Uijen GJH. Geometrical factors affecting the interindividual variability of the ECG and VCG. J Electrocardiol 2000;33(Suppl):219.

[4] Hoekema R, Uijen GJH, van Oosterom A. Geometrical aspects of the interindividual variability of multilead ECG recordings. IEEE Trans Biomed Eng 2001;48:551.

[5] Macleod RS, Ni Q, Punske B, Ershler PR, Yilmaz B, Taccardi B. Effects of heart position on the body-surface electrocardiogram. J Electrocardiol 2000;33(Suppl):229.

[6] De Ambroggi L, Negroni MS, Monza E, Bertoni T, Schwartz PJ. Dispersion of ventricular repolarization in the long QT syndrome. Am J Cardiol 1991;68:614.

[7] De Ambroggi L, Aime E, Ceriotti C, Rovida M, Negroni S. Mapping of ventricular repolarization potentials in patients with arrhythmogenic right ventricular dysplasia: principal component analysis of the ST-T waves. Circulation 1997;96(12):4314.

[8] Corlan AD, De Ambroggi L. New quantitative methods of ventricular repolarization analysis in patients with left ventricular hypertrophy. Ital Heart J 2000;1(8):542.

[9] Corlan AD, Macfarlane PW, De Ambroggi L. Gender differences in stability of the instantaneous patterns of body surface potentials during ventricular repolarisation. Med Biol Eng Comput 2003; 41:536.

[10] Corlan AD, Macleod RS, De Ambroggi L. Low variability of autocorrelation maps with intrathoracic heart position. Int J Bioelectromag 2003;5:139.

[11] Abildskov JA, Burgess MJ, Lux RL, Wyatt R, Vincent M. The expression of normal ventricular repolarization in the body surface distribution of T potentials. Circulation 1976;54:901.

[12] Gulrajani R, Roberge FA, Mailloux GE. The forward problem of electrocardiography, vol 3. Oxford: Pergamon Press; 1989. p. 202 [chapter 8].

[13] Barnard A, Duck IM, Lynn MS. The application of electromagnetic theory in electrocardiology. I derivation of the integral equations. Biophys J 1967;7:443.

[14] Hoekema R, Uijen GJ, Stilli D, van Oosterom A. Lead system transformation of body surface map data. J Electrocardiol 1998;31:71.

[15] Corlan AD, De Ambroggi L. Autocorrelation maps—a new method for the analysis of repolarization potentials. Electrocardiology, '2001, Sao Paolo; 2002. p. 35.

[16] Corlan AD, Corlan R, De Ambroggi L. Variability of simulated ECG autocorrelation maps with electrode placement. Int J Bioelectromag 2002;4:347.

[17] Geselowitz DB, Miller WT. A bidomain model for anisotropic cardiac muscle. Ann Biomed Eng 1983;11:191.